Jurnal Teknologi

Full Paper

CYTOTOXICITY AND IN-SILICO STUDY OF *Piper aduncum* EXTRACT TO INHIBIT BREAST CANCER CELL GROWTH

Jantje Wiliem Souhaly, Rarastoeti Pratiwi, Laurentius Hartanto Nugroho, Tri Rini Nuringtyas*

Faculty of Biology, Gadjah Mada University, Yogyakarta, Indonesia

Article history
Received
25 March 2025
Received in revised form
16 October 2025
Accepted
18 December 2025
Published Online
29 August 2026

*Corresponding author
tririni@ugm.ac.id

Graphical abstract

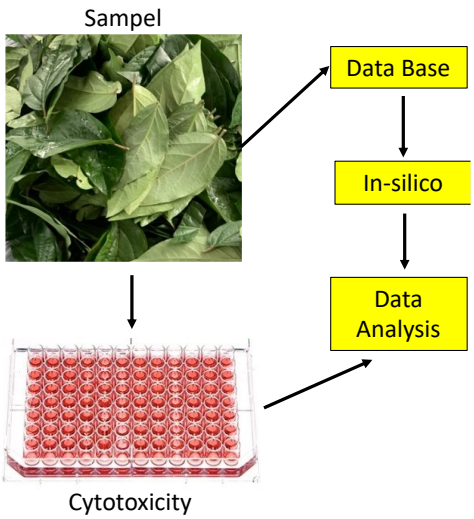

Abstract

Breast cancer is the most prevalent cancer among women worldwide and a leading cause of cancer-related deaths. *Piper aduncum* is a tropical plant recognized for various potential medicinal properties, such as anti-breast cancer. This study aims to investigate the anti-breast cancer potential of bioactive compounds found in *P. aduncum* leaf ethanolic extract by measuring of cytotoxicity and using a computational approach. Analysis of cytotoxic using MTT assay. Information on active compounds was collected from the KNApSAcK database. Druglikeness, Pa, and Toxicity class were analyzed by using ADMET, Way2Drug, and Protox II. AutoDock vina was used to simulate the docking of chemicals with their protein targets. The cytotoxic analysis showed that the ethanolic extract of *P. aduncum* have IC_{50} values 105.75 µg/mL. *P. aduncum* contains 21 bioactive compounds. Methyl 2,2-dimethyl-8-(3'-methyl-2'-butenyl)-2H-1-chromene-6-carboxylate, 2,2-Dimethyl-8-prenylchromene 6-carboxylic acid, Methyl 2,2-dimethyl-2H-1-chromene-6-carboxylate, Anofinic acid, Asebogenin, Cardamomin were predicted to exhibit anti-breast cancer activities. Meanwhile, anofinic acid displayed the potential interaction with RAC1. In conclusion, as indicated by computational analysis, *P. aduncum* leaf has high potential as an anti-breast cancer agent by inhibiting protein RAC1.

Keywords: Breast Cancer, *Piper aduncum*, Cytotoxicity, Computational Analysis, RAC1 Protein

1.0 INTRODUCTION

The case of cancer is increasing rapidly, affecting millions of people worldwide [1]. As the second-highest number of deaths globally, many researchers are focusing on the exploration of effective treatments. Despite significant advancements in this field, only a limited number of cancer drugs have successfully progressed through clinical trials [2]. Cancer cells vary widely and are classified based on genetic mutations such as colon, lung, and breast cancer [3]. Among these, breast cancer is the second most common cancer overall and is prevalent in women [4]. Treatment strategies must require different drugs depending on the specific characteristics of the cancer cells. Consequently, natural compounds from plants, including Piper aduncum, are being investigated for their potential anticancer properties.

Piper aduncum is an invasive plant from the genus of Piper. This plant has been used as traditional medicine for

therapeutic properties such as antimicrobial and anti-inflammatory. Also, the present studies described that active compounds from this plant have potential in cancer therapy [5–7]. Extracts from *P. aduncum* have been reported in several investigations to have cytotoxic effects on a variety of cancer cell lines, including breast, colon, and lung cancer [8, 9]. These effects include induction of apoptosis, cell proliferation inhibition, and metastatic suppression [10].

Nevertheless, the molecular mechanisms that regulate cancer growth are still unknown. In-silico analysis is a practical approach for early investigations of anticancer potential bioactive chemicals in *P. aduncum*. This strategy is critical to identifying new therapeutic molecules by predicting their cellular and molecular functions [11]. The current study analyzed the potential of the compound *P. aduncum* as an inhibitor of Ras-related C3 botulinum toxin substrate 1 (RAC1). RAC1 is a key regulator of the actin cytoskeleton, cell proliferation, migration, and survival [12–15]. Dysregulation of RAC1 activity has led to cancer progression, metastasis, and resistance to apoptosis [16–18]. Consequently, targeting RAC1 provides a potential approach for cancer treatment. Inhibition of this target may cause a synergistic effect, increasing therapy efficacy.

2.0 METHODOLOGY

2.1 Sample Collection and Extraction

Samples of *P. aduncum* leaf were obtained from Merapi Farma Yogyakarta, Indonesia. Plant species were identified by the Laboratory of Plant Systematic Biology, Gadjah Mada University, Yogyakarta, Indonesia. The raw materials were dried in the air space with a black net for around four to five days and blended to become powder. About 10 g of powder was extracted with 200 ml ethanol 96% using a Soxhlet extractor at 50^{0}C until the filtrate was clear. A rotary evaporator retrieved the crude extract. The obtained extract was put in the oven at 50^{0}C and, for future analysis, was stored at 4^{0}C.

2.2 Preparation of Cell Culture

T47D and Vero cell line was obtained from Cancer Chemoprevention Research Center (CCRC) Faculty of Pharmacy, Gadjah Mada University, Indonesia. Cells were grown in 25cm^2 tissue culture flask with complete media (Roswell Park Memorial Institute 1640 (elabscience) + 10% Fetal Bovine Serum (Gibco, USA) + 1% Penicillin streptomycin (elabscience) and incubate at 37^{0}C, 5% CO_2. The cells were observed under the inverted microscope, and after 80% confluent, harvest cells with add 300 µl trypsin solution (elabscience) for 5 min to detach cells, and 2 mL complete media was added to the flask. Furthermore, the subculture is added to a new well plate for treatment.

2.3 MTT Assay

The T47D cells were seeded in 96 well plates and incubated at 24h, 37^{0}C, 5% CO_2. The cells were treated with concentrations 400, 200, 100, 50, and 25 µg/mL. After 24h, the culture medium was discarded and washed by Phosphate Buffered Saline (Biorad). Replaced with medium containing MTT (cayman) solution 100 µl into each well; incubated for 4h at 37^{0}C, 5% CO_2. After discarding the medium MTT, add 100 µl of DMSO to each well to dissolve the formazan crystals. Incubate for ten minutes at room temperature. The absorbance was measured using an ELISA reader at a wavelength of 595. The IC50 values were calculated by linear regression of the data from cell viability percentage [19].

2.4 Compounds Collection

The compounds of *P. aduncum* were collected from the KNApSAcK database [20]. We also observed the previous studies; nevertheless, several compounds were included in the database. The 3D structures of compounds were retrieved from the PubChem database (https://pubchem.ncbi.nlm.nih.gov/). Furthermore, this structure was carried out using Autodock Vina for molecular docking.

2.5 Prediction of Druglikeness

Drug likeness was used to understand the absorption, distribution, and metabolism of the molecules inside the body (www.swissadme.ch) [21]. Additionally, The pharmacokinetic properties of the molecule were determined based on several rules such as Lipinski [22], Ghose [23], Veber [24], Egan [25], and Muegge [26]. The rationale behind these rules is that compounds suitable for these criteria are more likely to possess good pharmacokinetics.

2.6 Structure-Activity Relationship (SAR) and Toxicity Prediction

The way2drug pass online web server (https://www.way2drug.com/passonline/) was used to investigate the associations between the chemical structure of a molecule and biological properties. SMILES structure of molecules from the PubChem database were analyzed for the potential as anticancer activity. Several parameters related to cancer, such as apoptosis agonists [27], MMP9 expression inhibitors [28], antineoplastic [29], proliferative disease treatment agents [30], caspase-3 stimulants and caspase-8 stimulants [31]. Additionally, the prediction of the potential toxicity of chemical compounds was performed by ProTox-II webserver (parameter toxicity class, mutagenicity, carcinogenicity, cytotoxicity, and immunotoxicity) [32, 33].

2.7 Molecular Docking

Investigating interactions between a potential drug molecule and its biological target at the molecular level uses molecular docking. The 3D structure for RAC1 (PDB ID: 5N6O) [34]. Remove water molecules, cofactors, ions, and contaminants molecules from the protein structure that are not involved in ligand binding during the docking process using Biovia Discovery

Studio [35]. Interaction between ligand and receptor was performed using AutoDock Vina integrated into the PyRx [36]. The three-dimensional inhibitor compound collected from the PubChem database to protein RAC1 is NSC23766 (CID: 409805) [37]. *Native ligands* of protein were separated using AutodockTools and run docking in the binding site on the receptor protein to predict their interaction and affinity. The docking results were analyzed by Biovia Discovery Studio [35].

3.0 RESULTS AND DISCUSSION

3.1 Cytotoxicity Activity of *P. aduncum*

The cytotoxic activity demonstrated by the extracts was dependent on the dosage. Significant variations were noticed at specific treatment levels. Figure 1A shows the morphological changes of T47D cells treated with *P. aduncum* extracts. The difference in concentration shows a different picture when observed with an inverted microscope compared to untreated cells. At concentrations of 25 and 50 µg/mL, cancer cells proliferate and attach at the base of the flask. Cells proliferate, with little space between one cell and another; consequently, there is almost no difference from the untreated cells. While at the concentrations of 400 and 200 µg/mL, cells look less developed, and even there is no visible cell growth. It is also demonstrated by the low absorption value. In another case, in a dosage of 100 µg/mL, the cells look visible in small groups compared to 25 and 50 µg/mL The test also evaluates to non-target cell (Vero cells), as shown in Figure 1B.

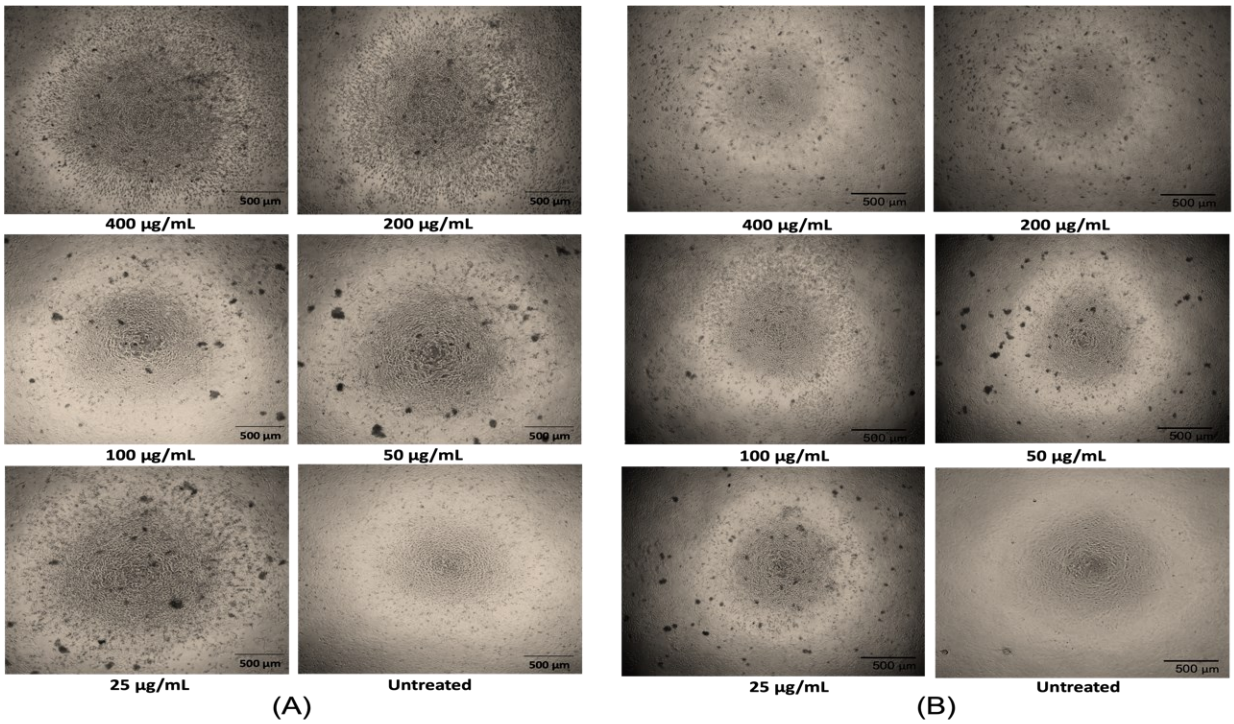

Figure 1 Microscopic image of cells captured at 10x magnification for visualizing morphological cell. (A) The T47D cells after treated with deferent dose for 24h (B) The Vero cells after treated with deferent dose for 24h. the arrow indicated cell death and black fill arrow is residue of extract

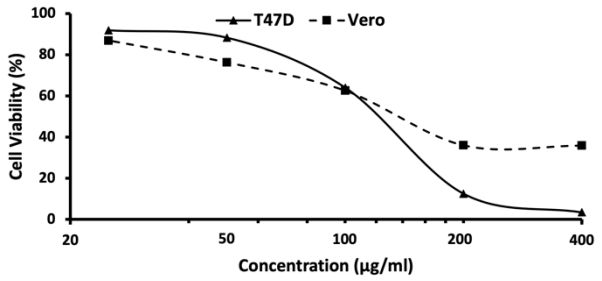

Figure 2 Dose response curve of extract *Piper aduncum* against T47D cells

The effective dosage has been determined by the concentration-response curve. The cells with lower concentrations described the highest cell viability (Figure 2). Table 1 shows the percentage of viability for each plate.

Table 1 Percentage viability of T47D cells on each plate

Plate	400 µg/ml	200 µg/ml	100 µg/ml	50 µg/ml	25 µg/ml
T47D	6.79%	12.24%	65.75%	92.30%	90.29%
	6.93%	12.52%	63.46%	87.13%	91.72%
	5.78%	12.81%	62.88%	85.41%	93.59%
Vero	36.69%	38.76%	66.34%	73.18%	90.39%
	36.90%	31.92%	64.47%	86.86%	76.91%
	34.00%	37.31%	56.80%	68.62%	93.29%

According to the National Cancer Institute (NCI) plant screening program, a crude extract is classified as high, moderate, weak and no cytotoxic activity [38]. In this research the IC_{50} value of the *P. aduncum* extract is 105.75 µg/mL (Table 2).

Table 2 IC_{50} value

	IC_{50} (µg/mL) ± SD	
Extract	**T47D**	**Vero**
Piper aduncum	105.75 ± 2.43	157.87 ± 12.54

Note: ±SD; n = 3; $p < 0.05$.

This suggests that the extracts exhibit moderate cytotoxic activity and may be suitable as potential anti-cancer agents. Investigating drug interaction in multi-compounds is complicated because some compounds may show interaction with less specific activity and may reduce the toxicity of more potential to medicinal plants [39]. Thus, next investigations will be conducted to the potential compounds as anti-cancer.

3.2 Compounds in *P. aduncum*

According to the results of the KNApSAcK database, *Piper aduncum* has 23 compounds (Table 3).

Table 3. The bioactive compound of *P. aduncum*

No.	Compound	CID
1	Asbogomin[a]	442255
2	Piperaduncin B[f]	442455
3	2,2-Dimethyl-8-propylchromene-6-carboxylic acid[b]	441962
4	Dillapiol[d]	10231
5	Myristicin[e]	4276
6	Safrole[e]	5144
7	Nerolidol[d]	5284507
8	(-)-beta-Sitosterol[a]	222284
9	Piperaduncin C*	10370473
10	2',6'-Dihydroxy-4'-methoxychalcone*	606469
11	Cardamonin*	154162
12	2',6'-Dihydroxy-4'-methoxydihydrochalcone*	129564321
13	Piperaduncin A[f]	10480725
14	Methyllinderatin[h]	42607684
15	Adunctin A[a]	42607686
16	Adunctin B[a]	42607687
17	Adunctin C[a]	42607688
18	Adunctin D[a]	42607689
19	Adunctin E[a]	42607690
20	Anofinic acid[b]	5319235
21	Methyl 2,2-dimethyl-2H-1-chromene-6-carboxylate[b]	40768
22	Methyl 2,2-dimethyl-8-(3'-methyl-2'-butenyl)-2H-1-chromene-6-carboxylate	440623
23	3,5-Bis(3-methyl-2-butenyl)-4-methoxybenzoic acid[g]	53736091

The compounds contained in *P. aduncum* are majority dominated by three groups of compounds triterpenoids, chormenes, and chalcone. As a majority of the bioactive compound triterpenoids are Asebogenin, (-)-beta-Sitosterol, Adunctin A, B, C, D, E. The Chromenes compounds are 2,2-Dimethyl-8-prenylchromene 6-carboxylic acid, Piperaduncin C, Anofinic acid, Methyl 2,2-dimethyl-2H-1-chromene-6-carboxylate and Methyl 2,2-dimethyl-8-(3'-methyl-2'-butenyl)-2H-1-chromene-6-carboxylate. Furthermore, Chalcone compounds are 2',6'-Dihydroxy-4'-methoxychalcone, Cardamomin, 2',6'-Dihydroxy-4'-methoxydihydrochalcone. Additionally, two alkaloids (Piperaduncin B, Piperaduncin A), two essential oils (Dillapiol, Nerolidol), two Phenylpropene (Myristicin, Safrole), and one Benzoic acids (3,5-Bis(3-methyl-2-butenyl)-4-methoxybenzoic acid) and Flavonoid (Methyllinderatin) (Figure 3a).

3.3 Prediction of Druglikeness

Druglikeness refers to the characteristics of a compound that indicate its potential to become an orally active medicinal product in humans [40]. Several key parameters and rules are used for drug-likeness. Of the 21 compounds, nine compounds have characteristic of medicinal with violate specific to these rules (Figure 3b). For instance, piperaduncin B has a Molecular Weight (MW) >500, leading to a violation of one of Lipinski's rules. Compounds that violate two or more of the Lipinski Rule of Five criteria have been considered low drug ability [41]. Moreover, (-)-beta-Sitosterol, Piperaduncin C, and Piperaduncin A violate Ghose criteria for lipophilicity due to their WlogP values 5.6. When the WlogP value surpasses 5, it indicates high lipophilicity or low solubility, potentially affecting the compounds absorption within the body [42]. Future analysis will focus on evaluating the nine compounds (asebogenin, 2.2-Dimethyl-8-prenylchromene 6-carboxylic acid, dillapiole, 2',6'-Dihydroxy-4'-methoxychalcone, Cardamomin, 2',6'-Dihydroxy-4'-methoxydihydrochalcone, Anofinic acid, Methyl 2,2-dimethyl-2H-1-chromene-6-carboxylate, Methyl 2,2-dimethyl-8-(3'-methyl-2'-butenyl)-2H-1-chromene-6-carboxylate) that have druglike characteristic for analysis of probable bioactivity and predicting their activity in inhibiting breast cancer.

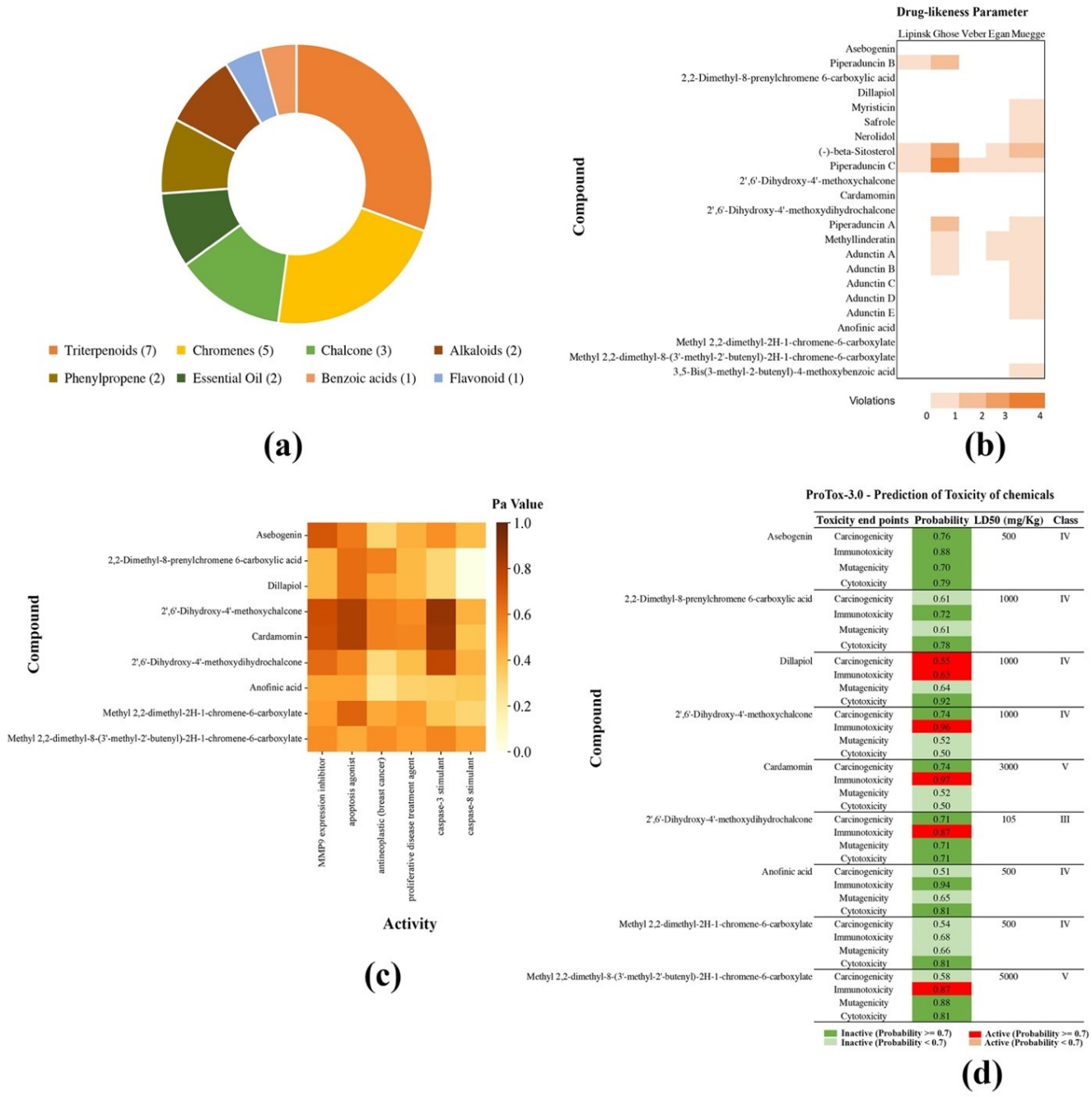

Figure 3: The bioactive compound contains in *P. aduncum*. (a) Groups of bioactive compounds. (b) Druglikeness rules of violations. (c) Structure-activity relationship (SAR) using PASS online. (d) The level of toxicity

3.4 Prediction Structure-Activity Relationship (SAR) and Toxicity Prediction

According to the PASS online results indicate that compounds Asebogenin, 2',6'-Dihydroxy-4'-methoxychalcone, and cardamoin were identified as having high potential as MMP9 expression inhibitors with Pa > 0.7 values. Furthermore, 2',6'-Dihydroxy-4'-methoxychalcone and Cardamomin exhibit the highest apoptosis agonist and also with 2',6'-Dihydroxy-4'-methoxydihydrochalcone having high activity as caspase 3 stimulant with Pa value more than 0.7 (Figure 3c). The probability to be active (Pa) score, which is higher than 0.7, suggests that the molecule has a high potential activity depending on the parameters [43]. Previous studies have shown that several of these bioactive chemicals have anticancer properties, while the molecular mechanism is not

completely clear. Cardomin can induce apoptosis and suppress proliferation in prostate cancer [44]. Research on the anticancer effect of these compounds is still limited. This study described how these compounds provide an anti-breast cancer effect.

The toxicity of nine potential active compounds was evaluated using the Pro-Tox server. Based on toxicity class, six compounds have toxicity class IV with an LD50 of 300–2000 mg/kg. Meanwhile, two compounds have toxicity class V with an LD50 of 3000 mg/kg. One compound with toxicity class III, an LD50 of 105 mg/kg (Figure 3d). According to the Globally Harmonised System (GHS), the toxicity class ranges from class I to VI based on the LD50 values in mice, with the highest class being VI (safety orally). In this study, most bioactive compounds fall into the toxicity class IV (harmful if swallowed). Compounds that fall into the class V represent that compound may be harmful if swallowed and may be toxic if swallowed on the class III [31]. The prediction of oral toxicity could help future analyses determine the safe dosage. In comparison to other compounds were relative safe, 2',6'-Dihydroxy-4'-methoxychalcone, cardomin, 2',6'-Dihydroxy-4'-methoxychalcone and Methyl 2,2-dimethyl-8-(3'-methyl-2'-butenyl)-2H-1-chromene-6-carboxylate have potential immunogenic also cardomin has potential carcinogenic properties.

3.4 Molecular Docking Analysis

The inhibition activity of nine compounds of *P. aduncum* against RAC1 was investigated using in-silico molecular docking. This study aimed to evaluate the activity of RAC1 inhibition based on the bonding form and interaction of the ligands on the receptor's active site (Figure 4). We also investigated the re-docking results of the native ligand and RAC1. Re-docking was conducted based on the lowest energy interaction between backbone atoms and the active region of RAC1, with a binding affinity of -9.4 kcal/mol. Additionally, NSC-23766, as an inhibitor of RAC1, was also compared with native ligand (Figure 5). Compounds in *P. aduncum* exhibited lower binding affinity than native ligands. However, six compounds showed a more potent binding affinity to RAC1 than a known inhibitor (NSC-23766; -7 kcal/mol; Figure 4).

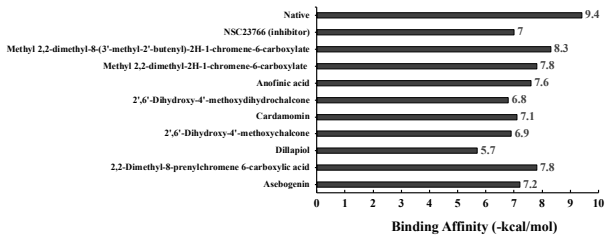

Figure 4 Binding affinity of receptor (RAC1)-Ligand (control and all compounds) (-kcal/mol)

Further investigation focused on the compounds with the highest binding affinity to inhibitors and their interaction with RAC1's active site. This analysis shows a crucial component of analyzing the ability of a compound to inhibit RAC1. Several types of interaction via amino acid residues between ligand native and RAC1 are shown in Table 4. There were 15 hydrogen bond and three hydrophobic interactions. The involvement of amino acid residues in this interaction was ALA13, VAL14, LYS16, GLY15, THR17, CYS18, and CYS116. These residues were considered to be the key amino acid residues. These residues were considered to be the key amino acid residues. It can be suggested that the RAC1 protein plays a crucial function in regulating the stability of protein-ligan interactions because of the total number of hydrogen bonds. NSC-23766 and RAC1 formed two hydrogen bonds (conventional hydrogen bond and carbon hydrogen bond), other (Pi-sulfur), and 13 hydrophobic bonds (seven alkyl and six Pi-alkyl). Meanwhile, the hydrogen bond was THR17 and ASP118. The Methyl 2,2-dimethyl-8-(3'-methyl-2'-butenyl)-2H-1-chromene-6-carboxylate against RAC1 formed two hydrogen bonds (two conventional hydrogen bond) and four hydrophobic bonds (three alkyl and a Pi-alkyl) with hydrogen bond was THR17. Compound 2,2-Dimethyl-8-prenylchromene 6-carboxylic acid forms five hydrogen bonds (four conventional hydrogen bond and a Pi-Donor hydrogen bond) and five hydrophobic bonds (five alkyl) ALA13, LYS16, ASP57, THR58 and GLY60. Meanwhile, Methyl 2,2-dimethyl-2H-1-chromene-6-carboxylate forms a hydrogen bond (a conventional hydrogen bond) and three hydrophobic bonds (an alkyl and two Pi-alkyl). Beside 2,2-Dimethyl-8-prenylchromene 6-carboxylic acid compound, anofinic acid and asebogenin have more hydrogen bonds compared to other with 6, 5 hydrogen bonds, respectively.

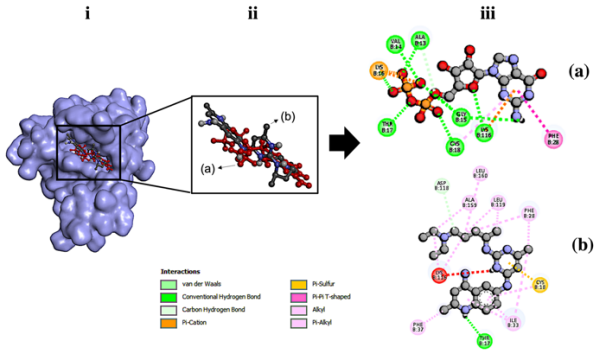

Figure 5. The visualization of molecular docking between RAC1 with (a) *native ligand* and (b) NSC-23766. At the left (i) RAC1 presented in blue surface with ligands presented. In the middle (ii) Position of ligands bind on the same side (iii) 2D structure of ligand-protein complex

To assess the potential of ligands from *P. aduncum* for inhibiting RAC1, the analysis of the binding site between RAC1 and ligands was conducted. The interaction of ligand docking was compared to the binding site of *native ligands* and NSC-23766 as an inhibitor of RAC1. A *native ligand* is a molecule that naturally binds to a specific receptor or protein under physiological conditions [45]. This binding is often characterized by high specificity and affinity, playing a crucial role in the normal biological function of the protein [46]. The docking results showed that compound Methyl 2,2-dimethyl-8-(3'-methyl-2'-butenyl)-2H-1-chromene-6-carboxylate, 2,2-Dimethyl-8-prenylchromene 6-carboxylic acid, Anofinic acid, and Cardomin demonstrates potential as a competitive inhibitor because it directly binds to the protein at the active site (Figure 6).

Previous research has shown that *P. aduncum* consists of chemical compounds with anticancer activity and has been recognized as effective agents for human health [5]. However, the mechanisms of action explaining the anticancer characteristics remain unknown. RAC1 has been used as a target in cancer treatment [47]. The protein is a receptor that controls cell growth, migration, proliferation, and angiogenesis (Figure 7) [47–50]. Compounds *from P. aduncum* have a limited mode of action as anticancer treatments. A docking study was carried out to investigate the potential of compounds from *P. aduncum* as anticancer therapies by inhibiting RAC1.

Table 4 Detailed interactions between RAC1 with bioactive compounds

Compound	Name	Distance	Category	Types
Native	B:LYS16:HZ2 - N:UNK1:O	1.86912	Hydrogen Bond; Electrostatic	Salt Bridge; Attractive Charge
	B:LYS16:NZ - N:UNK1:O	4.56218	Electrostatic	Attractive Charge
	B:ALA13:HN - N:UNK1:O	1.9234	Hydrogen Bond	Conventional Hydrogen Bond
	B:VAL14:HN - N:UNK1:O	2.24335	Hydrogen Bond	Conventional Hydrogen Bond
	B:GLY15:HN - N:UNK1:O	2.69794	Hydrogen Bond	Conventional Hydrogen Bond
	B:GLY15:HN - N:UNK1:O	2.02595	Hydrogen Bond	Conventional Hydrogen Bond
	B:LYS16:HN - N:UNK1:O	2.27298	Hydrogen Bond	Conventional Hydrogen Bond
	B:LYS16:HZ1 - N:UNK1:O	2.42836	Hydrogen Bond	Conventional Hydrogen Bond
	B:THR17:HN - N:UNK1:O	1.75687	Hydrogen Bond	Conventional Hydrogen Bond
	B:CYS18:HN - N:UNK1:O	2.11414	Hydrogen Bond	Conventional Hydrogen Bond
	B:LYS116:HZ1 - N:UNK1:O	2.80739	Hydrogen Bond	Conventional Hydrogen Bond
	B:LYS116:HZ2 - N:UNK1:O	2.56723	Hydrogen Bond	Conventional Hydrogen Bond
	N:UNK1:H - B:GLY15:O	2.68086	Hydrogen Bond	Conventional Hydrogen Bond
	B:ALA13:HA - N:UNK1:O	2.7056	Hydrogen Bond	Carbon Hydrogen Bond
	B:ALA13:HA - N:UNK1:O	2.92148	Hydrogen Bond	Carbon Hydrogen Bond
	B:LYS16:HE1 - N:UNK1:O	2.76378	Hydrogen Bond	Carbon Hydrogen Bond
	B:LYS116:NZ - N:UNK1	4.3299	Electrostatic	Pi-Cation
	B:PHE28 - N:UNK1	5.12637	Hydrophobic	Pi-Pi T-shaped
	N:UNK1 - B:CYS18	5.02616	Hydrophobic	Pi-Alkyl
	N:UNK1 - B:LYS116	3.94489	Hydrophobic	Pi-Alkyl
NSC23766	N:UNK1:HN - B:THR17:OG1	2.06398	Hydrogen Bond	Conventional Hydrogen Bond
	N:UNK1:C - B:ASP118:OD1	3.72028	Hydrogen Bond	Carbon Hydrogen Bond
	B:CYS18:SG - N:UNK1	4.2365	Other	Pi-Sulfur
	B:LYS116 - N:UNK1	4.16101	Hydrophobic	Alkyl
	B:ALA159 - N:UNK1:C	3.61341	Hydrophobic	Alkyl
	N:UNK1:C - B:ILE33	4.79191	Hydrophobic	Alkyl
	N:UNK1:C - B:LEU119	5.07804	Hydrophobic	Alkyl
	N:UNK1 - B:LEU119	5.03702	Hydrophobic	Alkyl
	N:UNK1 - B:LEU160	4.82398	Hydrophobic	Alkyl

Compound	Name	Distance	Category	Types
	N:UNK1:C - B:LYS116	4.06195	Hydrophobic	Alkyl
	B:PHE28 - N:UNK1:C	5.44259	Hydrophobic	Pi-Alkyl
	B:PHE28 - N:UNK1	5.33941	Hydrophobic	Pi-Alkyl
	B:PHE37 - N:UNK1:C	4.44805	Hydrophobic	Pi-Alkyl
	N:UNK1 - B:ILE33	4.09811	Hydrophobic	Pi-Alkyl
	N:UNK1 - B:CYS18	5.2957	Hydrophobic	Pi-Alkyl
	N:UNK1 - B:ILE33	4.13821	Hydrophobic	Pi-Alkyl
Methyl 2,2-dimethyl-8-(3'-methyl-2'-butenyl)-2H-1-chromene-6-carboxylate	B:THR17:HN – N:UNK1:O	1.95697	Hydrogen Bond	Conventional Hydrogen Bond
	N:UNK1:H – B:THR17:OG1	2.3322	Hydrogen Bond	Conventional Hydrogen Bond
	B:CYS18 – N:UNK1	5.08832	Hydrophobic	Alkyl
	B:ILE33 – N:UNK1	4.40981	Hydrophobic	Alkyl
	B:ILE33 – N:UNK1	3.96567	Hydrophobic	Alkyl
	N:UNK1 – B:ILE33	4.75684	Hydrophobic	Pi-Alkyl
2,2-Dimethyl-8-prenylchromene-6-carboxylic acid	B:LYS16:HZ1 – N:UNK1:O	2.28115	Hydrogen Bond	Conventional Hydrogen Bond
	B:GLY60:HN – N:UNK1:O	2.67976	Hydrogen Bond	Conventional Hydrogen Bond
	N:UNK1:H – B:ASP57:OD1	2.84984	Hydrogen Bond	Conventional Hydrogen Bond
	N:UNK1:H – B:THR58:O	2.02545	Hydrogen Bond	Conventional Hydrogen Bond
	B:ALA13:HN – N:UNK1	2.84240	Hydrogen Bond	Pi-Donor Hydrogen Bond
	B:ALA13 – N:UNK1:C	4.24690	Hydrophobic	Alkyl
	B:CYS18 – N:UNK1	5.13947	Hydrophobic	Alkyl
	B:ILE33 – N:UNK1	4.90514	Hydrophobic	Alkyl
	N:UNK1:C – B:CYS18	5.02027	Hydrophobic	Alkyl
	N:UNK1:C – B:ILE33	3.58507	Hydrophobic	Alkyl
Methyl 2,2-dimethyl-2H-1-chromene-6-carboxylate	N:UNK1:H – B:PRO34:O	2.58076	Hydrogen Bond	Conventional Hydrogen Bond
	N:UNK1:C – B:LYS16	4.43712	Hydrophobic	Alkyl
	B:PHE37 – N:UNK1:C	5.04011	Hydrophobic	Pi-Alkyl
	N:UNK1 – B:ILE33	4.92732	Hydrophobic	Pi-Alkyl
Anofinic acid	B:ALA13:HN - N:UNK1:O	2.59279	Hydrogen Bond	Conventional Hydrogen Bond
	B:VAL14:HN - N:UNK1:O	2.60671	Hydrogen Bond	Conventional Hydrogen Bond
	B:GLY15:HN - N:UNK1:O	2.00959	Hydrogen Bond	Conventional Hydrogen Bond
	B:LYS16:HN - N:UNK1:O	2.34198	Hydrogen Bond	Conventional Hydrogen Bond
	B:LYS16:HZ2 - N:UNK1:O	2.30497	Hydrogen Bond	Conventional Hydrogen Bond
	N:UNK1:H - B:THR17:OG1	2.03353	Hydrogen Bond	Conventional Hydrogen Bond
	B:CYS18 - N:UNK1	4.55061	Hydrophobic	Alkyl
	B:ILE33 - N:UNK1	4.66766	Hydrophobic	Alkyl
	N:UNK1 - B:CYS18	5.22591	Hydrophobic	Pi-Alkyl
	N:UNK1 - B:ILE33	4.64398	Hydrophobic	Pi-Alkyl
Asebogenin	B:LYS116:HZ2 - N:UNK1:O	2.34066	Hydrogen Bond	Conventional Hydrogen Bond
	B:LYS116:HZ2 - N:UNK1:O	2.98927	Hydrogen Bond	Conventional Hydrogen Bond
	B:ALA159:HN - N:UNK1:O	2.03567	Hydrogen Bond	Conventional Hydrogen Bond
	N:UNK1:H - B:ASP118:OD2	2.12360	Hydrogen Bond	Conventional Hydrogen Bond
	N:UNK1:C - B:GLY15:O	3.53313	Hydrogen Bond	Carbon Hydrogen Bond
	B:PHE28 - N:UNK1	5.22607	Hydrophobic	Pi-Pi T-shaped
	N:UNK1 - N:UNK1	5.77089	Hydrophobic	Pi-Pi T-shaped
	B:ALA159 - N:UNK1:C	3.50620	Hydrophobic	Alkyl
	N:UNK1:C - B:LEU19	4.89662	Hydrophobic	Alkyl
	N:UNK1:C - B:LYS116	4.91332	Hydrophobic	Alkyl
	N:UNK1 - B:CYS18	5.32357	Hydrophobic	Pi-Alkyl

Compound	Name	Distance	Category	Types
	N:UNK1 - B:LYS116	3.70251	Hydrophobic	Pi-Alkyl
	N:UNK1 - B:ALA159	4.90968	Hydrophobic	Pi-Alkyl
	N:UNK1 - B:CYS18	5.26087	Hydrophobic	Pi-Alkyl
Cardamomin	B:VAL14:HN - N:UNK1:O	2.59538	Hydrogen Bond	Conventional Hydrogen Bond
	B:LYS16:HZ2 - N:UNK1:O	2.42424	Hydrogen Bond	Conventional Hydrogen Bond
	N:UNK1:H - B:THR58:O	2.36468	Hydrogen Bond	Conventional Hydrogen Bond
	N:UNK1 - B:LYS16	5.49260	Hydrophobic	Pi-Alkyl

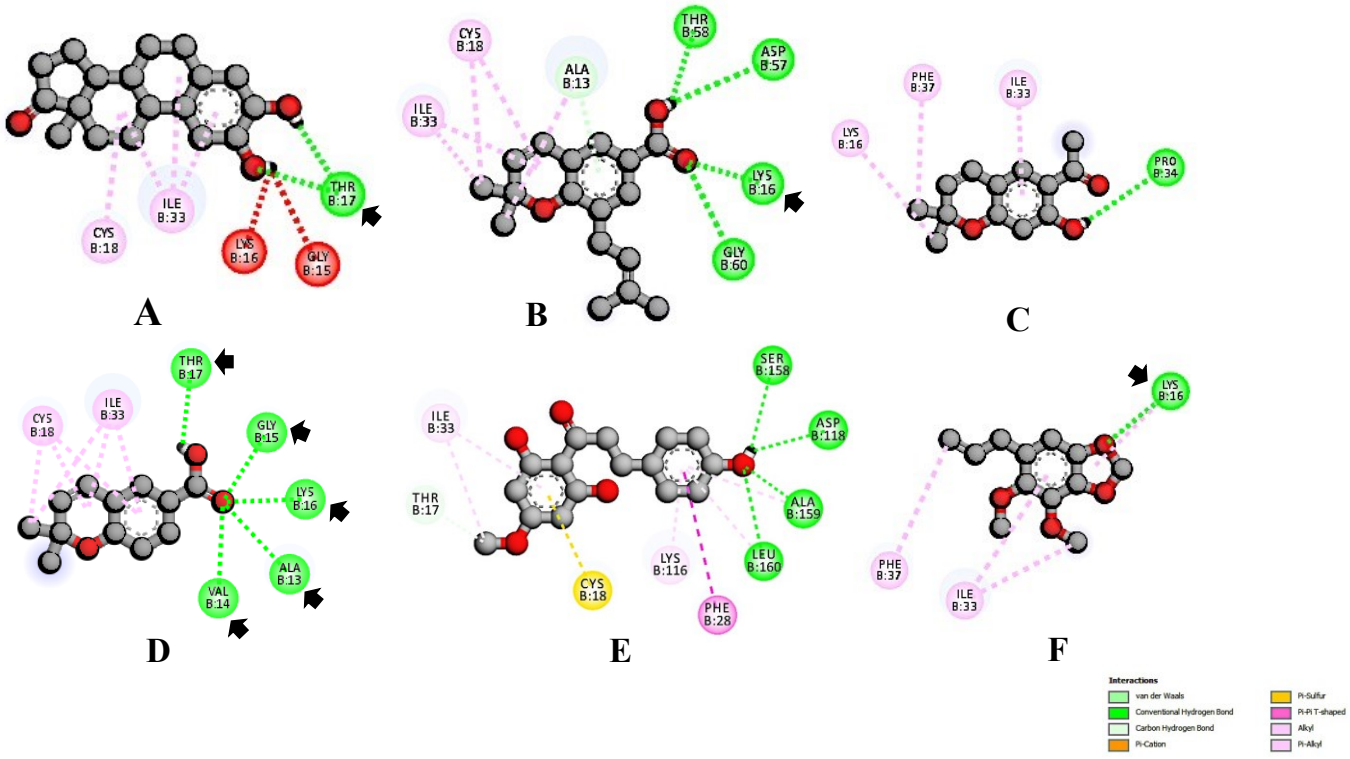

Figure 6 2D structure protein binding interaction with the phytochemical of *P. aduncum*. (A) Methyl 2,2-dimethyl-8-(3'-methyl-2'-butenyl)-2H-1-chromene-6-carboxylate; (B) 2,2-Dimethyl-8-prenylchromene 6-carboxylic acid; (C) Methyl 2,2-dimethyl-2H-1-chromene-6-carboxylate; (D) Anofinic acid; (E) Asebogenin; (F) Cardamomin. The arrow indicated that ligand binding to a crucial amino acid residue with hydrogen bonds

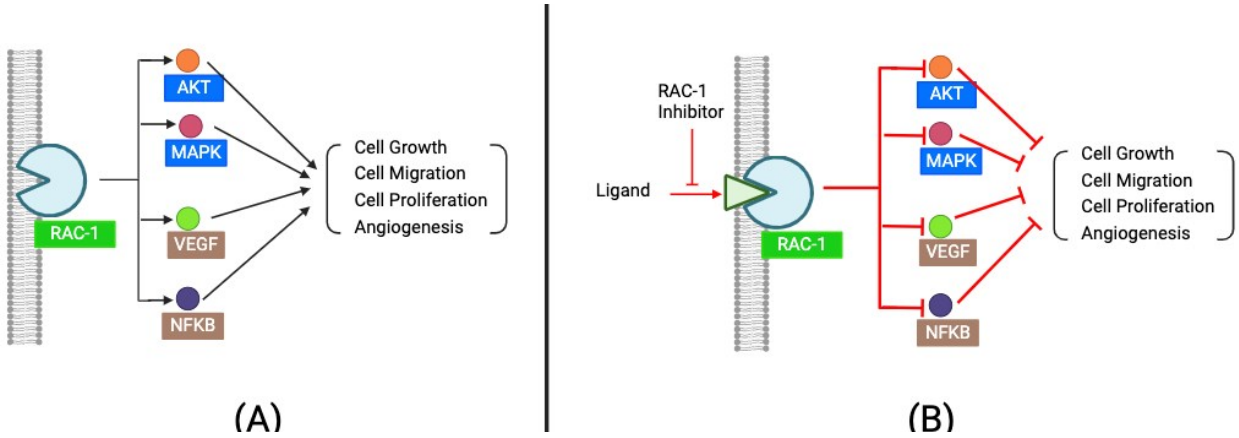

Figure 7 Anticancer mechanism of compounds *P. aduncum* through inhibition of RAC1 (A) RAC1 increases cell growth, cell migration, cell proliferation and angiogenesis (B) Inhibition of the RAC1 protein may lead to decreased proliferation, migration of cells, and angiogenesis, which may lead to apoptosis

In conclusion, this study demonstrates that the extract of *P. aduncum* exhibits significant cytotoxicity against the T47D breast cancer cell line. Through an integrated cytotoxicity and *in silico* approach, we have identified six potential bioactive compounds Methyl 2,2-dimethyl-8-(3'-methyl-2'-butenyl)-2H-1-chromene-6-carboxylate; 2,2-Dimethyl-8-prenyl chromene 6-carboxylic acid; Methyl 2,2-dimethyl-2H-1-chromene-6-carboxylate; Anofinic acid; Asebo genin; Cardamomin that likely contribute to activity of anticancer. The computation-nal analysis predicts that these compounds have a multi-target mechanism with several key pathways involved in breast cancer progression. While these *in silico* findings provide a valuable theoretical framework for the plant's mechanism of action, they remain predictive. Therefore, further experimental research should be conducted *in-vivo* or *in-vitro* to confirm their therapeutic potential.

Acknowledgement

The author is grateful to Lembaga Pengelolaan Dana Pendidikan (LPDP) for funding this research.

Conflicts of Interest

There are no potential conflicts of interest.

References

[1] Ferlay, J., I. Soerjomataram, R. Dikshit, S. Eser, C. Mathers, M. Rebelo, D. M. Parkin, D. Forman, and F. Bray. 2015. Cancer Incidence and Mortality Worldwide: Sources, Methods and Major Patterns in GLOBOCAN 2012. *International Journal of Cancer.* 136(5): E359–E386.

[2] Chary, K. V., and K. Pandian. 2017. Accelerated Approval of Drugs: Ethics versus Efficacy. *Indian Journal of Medical Ethics.* 2(4): 244–247.

[3] Pilié, P. G., A. M. Johnson, K. L. Hanson, M. E. Dayno, A. L. Kapron, E. M. Stoffel, and K. A. Cooney. 2017. Germline Genetic Variants in Men with Prostate Cancer and One or More Additional Cancers. *Cancer.* 123(20): 3925–3932.

[4] Bray, F., J. Ferlay, I. Soerjomataram, R. L. Siegel, L. A. Torre, and A. Jemal. 2018. Global Cancer Statistics 2018: GLOBOCAN Estimates of Incidence and Mortality Worldwide for 36 Cancers in 185 Countries. *A Cancer Journal for Clinicians.* 68(6): 394–424.

[5] Monzote, L., R. Scull, P. Cos, and W. N. Setzer. 2017. Essential Oil from *Piper aduncum*: Chemical Analysis, Antimicrobial Assessment, and Literature Review. *Medicines.* 4(3): 49.

[6] Thao, N. P., B. T. T. Luyen, W. Widowati, N. Fauziah, M. Maesaroh, T. Herlina, Z. Manzoor, I. Ali, Y. S. Koh, and Y. H. Kim. 2016. Anti-inflammatory Flavonoid C-Glycosides from *Piper aduncum* Leaves. *Planta Medica.* 82: 1475–1481.

[7] Wang, Y.-H., S. L. Morris-Natschke, J. Yang, H.-M. Niu, C.-L. Long, and K.-H. Lee. 2014. Anticancer Principles from Medicinal *Piper* (*Hu Jiao*) Plants. *Journal of Traditional and Complementary Medicine.* 4(1): 8–16.

[8] Mayanga-Herrera, A., S. Tapia-Rojas, A. Fukusaki-Yoshizawa, Á. Marcelo-Rodríguez, and J. Amiel-Pérez. 2020. Actividad Citotóxica de la Fracción Clorofórmica de *Piper aduncum* y Su Efecto en el Ciclo Celular en Líneas Celulares de Cáncer Gástrico. *Revista Peruana de Medicina Experimental y Salud Pública.* 37(3): 471–477.

[9] Arroyo-Acevedo, J., R. J. Chávez-Asmat, A. Anampa-Guzmán, R. Donaires, and J. Ráez-Gonzáles. 2015. Protective Effect of *Piper aduncum* Capsule on DMBA-Induced Breast Cancer in Rats. *Breast Cancer: Basic and Clinical Research.* 9: 41.

[10] Ferreira, A. K., P. L. de Sá-Júnior, K. F. M. Pasqualoto, R. A. de Azevedo, D. A. D. Câmara, A. S. Costa, C. R. Figueiredo, *et al.* 2014. Cytotoxic Effects of Dillapiole on MDA-MB-231 Cells Involve the Induction of Apoptosis through the Mitochondrial Pathway by Inducing Oxidative Stress while Altering the Cytoskeleton Network. *Biochimie.* 99: 195–207.

[11] Xia, X. 2017. Bioinformatics and Drug Discovery. *Current Topics in Medicinal Chemistry.* 17(15): 1709–1726.

[12] Vega, F. M., and A. J. Ridley. 2008. Rho GTPases in Cancer Cell Biology. *FEBS Letters.* 582(14): 2093–2101.

[13] Bosco, E. E., J. C. Mulloy, and Y. Zheng. 2009. Rac1 GTPase: A 'Rac' of All Trades. *Cellular and Molecular Life Sciences.* 66(3): 370–374.

[14] Gastonguay, A., T. Berg, A. D. Hauser, N. Schuld, E. Lorimer, and C. L. Williams. 2012. The Role of Rac1 in the Regulation of NF-κB Activity, Cell Proliferation, and Cell Migration in Non-Small Cell Lung Carcinoma. *Cancer Biology & Therapy.* 13(8): 647–656.

[15] Marei, H., and A. Malliri. 2017. GEFs: Dual Regulation of Rac1 Signaling. *Small GTPases.* 8(2): 90–99.

[16] Guo, Y., J. Zhu, X. Wang, R. Li, K. Jiang, S. Chen, J. Fan, L. Xue, and D. Hao. 2019. Orai1 Promotes Osteosarcoma Metastasis by Activating the Ras–Rac1–WAVE2 Signaling Pathway. *Medical Science Monitor.* 25: 9227–9236.

[17] Swaminathan, K., A. Campbell, V. Papalazarou, F. Jaber-Hijazi, C. Nixon, E. McGhee, D. Strathdee, O. J. Sansom, and L. M. Machesky. 2021. The RAC1 Target NCKAP1 Plays a Crucial Role in the Progression of *Braf;Pten*-Driven Melanoma in Mice. *Journal of Investigative Dermatology.* 141(3): 628–637.e15.

[18] Zhou, H.-C., C.-X. Liu, W.-D. Pan, L.-R. Shang, J.-L. Zheng, B.-Y. Huang, J.-Y. Chen, L. Zheng, J.-H. Fang, and S.-M. Zhuang. 2021. Dual and Opposing Roles of the Androgen Receptor in VETC-Dependent and Invasion-Dependent Metastasis of Hepatocellular Carcinoma. *Journal of Hepatology.* 75(4): 900–911. https://doi.org/10.1016/j.jhep.2021.05.021.

[19] Nur, R. M., and L. H. Nugroho. 2017. Cytotoxic Activities of Fractions from *Dioscorea bulbifera* L. Chloroform and Methanol Extracts on T47D Breast Cancer Cells. *Pharmacognosy Journal.* 10(1): 33–38. https://doi.org/10.5530/pj.2018.1.7.

[20] Afendi, F. M., T. Okada, M. Yamazaki, A. Hirai-Morita, Y. Nakamura, K. Nakamura, S. Ikeda, H. Takahashi, M. Altaf-Ul-Amin, L. K. Darusman, K. Saito, and S. Kanaya. 2012. KNApSAcK Family Databases: Integrated Metabolite–Plant Species Databases for Multifaceted Plant Research. *Plant and Cell Physiology.* 53(2): e1. https://doi.org/10.1093/pcp/pcr165.

[21] Daina, A., O. Michielin, and V. Zoete. 2017. SwissADME: A Free Web Tool to Evaluate Pharmacokinetics, Drug-Likeness and Medicinal Chemistry Friendliness of Small Molecules. *Scientific Reports.* 7(1): 42717. https://doi.org/10.1038/srep42717.

[22] Lipinski, C. A., F. Lombardo, B. W. Dominy, and P. J. Feeney. 2001. Experimental and Computational Approaches to Estimate Solubility and Permeability in Drug Discovery and Development Settings. *Advanced Drug Delivery Reviews.* 46(1–3): 3–26. https://doi.org/10.1016/S0169-409X(00)00129-0.

[23] Ghose, A. K., V. N. Viswanadhan, and J. J. Wendoloski. 1999. A Knowledge-Based Approach in Designing Combinatorial or Medicinal Chemistry Libraries for Drug Discovery. 1. A Qualitative and Quantitative Characterization of Known Drug Databases. *Journal of*

Combinatorial Chemistry. 1(1): 55–68. https://doi.org/10.1021/cc9800071.
[24] Veber, D. F., S. R. Johnson, H.-Y. Cheng, B. R. Smith, K. W. Ward, and K. D. Kopple. 2002. Molecular Properties That Influence the Oral Bioavailability of Drug Candidates. *Journal of Medicinal Chemistry*. 45(12): 2615–2623. https://doi.org/10.1021/jm020017n.
[25] Egan, W. J., K. M. Merz Jr., and J. J. Baldwin. 2000. Prediction of Drug Absorption Using Multivariate Statistics. *Journal of Medicinal Chemistry*. 43(21): 3867–3877. https://doi.org/10.1021/jm000292e.
[26] Muegge, I., S. L. Heald, and D. Brittelli. 2001. Simple Selection Criteria for Drug-like Chemical Matter. *Journal of Medicinal Chemistry*. 44(12): 1841–1846. https://doi.org/10.1021/jm015507e.
[27] Hu, S., Y. Xu, L. Meng, L. Huang, and H. Sun. 2018. Curcumin Inhibits Proliferation and Promotes Apoptosis of Breast Cancer Cells. *Experimental and Therapeutic Medicine*. 16(2): 1266–1272. https://doi.org/10.3892/etm.2018.6345.
[28] Merdad, A., S. Karim, H.-J. Schulten, A. Dallol, A. Buhmeida, F. Al-Thubaity, M. A. Gari, A. G. Chaudhary, A. M. Abuzenadah, and M. H. Al-Qahtani. 2014. Expression of Matrix Metalloproteinases (MMPs) in Primary Human Breast Cancer: MMP-9 as a Potential Biomarker for Cancer Invasion and Metastasis. *Anticancer Research*. 34(3): 1355–1366.
[29] Kubatka, P., A. Kapinová, P. Kružliak, M. Kello, D. Výbohová, K. Kajo, M. Novák, M. Chripková, M. Adamkov, M. Péč, J. Mojžiš, B. Bojková, M. Kassayová, N. Stollárová, and D. Dobrota. 2015. Antineoplastic Effects of *Chlorella pyrenoidosa* in the Breast Cancer Model. *Nutrition and Cancer*. 67(4). https://doi.org/10.1080/01635581.2015.1015741.
[30] Okoth, C., M. Galukande, J. Jombwe, and D. Wamala. 2013. Benign Proliferative Breast Diseases among Female Patients at a Sub-Saharan Africa Tertiary Hospital: A Cross-Sectional Study. *BMC Surgery*. 13(1): 9. https://doi.org/10.1186/1471-2482-13-9.
[31] Pu, X., S. J. Storr, Y. Zhang, E. A. Rakha, A. R. Green, I. O. Ellis, and S. G. Martin. 2017. Caspase-3 and Caspase-8 Expression in Breast Cancer: Caspase-3 Is Associated with Survival. *Apoptosis*. 22(3): 357–368. https://doi.org/10.1007/s10495-016-1335-5.
[32] Drwal, M. N., P. Banerjee, M. Dunkel, M. R. Wettig, and R. Preissner. 2014. ProTox: A Web Server for the *In Silico* Prediction of Rodent Oral Toxicity. *Nucleic Acids Research*. 42(W1): W53–W58. https://doi.org/10.1093/nar/gku401.
[33] Banerjee, P., A. O. Eckert, A. K. Schrey, and R. Preissner. 2018. ProTox-II: A Webserver for the Prediction of Toxicity of Chemicals. *Nucleic Acids Research*. 46(W1): W257–W263. https://doi.org/10.1093/nar/gky318.
[34] Ferrandez, Y., W. Zhang, F. Peurois, L. Akendengué, A. Blangy, M. Zeghouf, and J. Cherfils. 2017. Allosteric Inhibition of the Guanine Nucleotide Exchange Factor DOCK5 by a Small Molecule. *Scientific Reports*. 7(1): 14409. https://doi.org/10.1038/s41598-017-14608-8.
[35] Dassault Systèmes BIOVIA. 2019. *Discovery Studio Modeling Environment*. San Diego, CA: Dassault Systèmes BIOVIA.
[36] Trott, O., and A. J. Olson. 2010. AutoDock Vina: Improving the Speed and Accuracy of Docking with a New Scoring Function, Efficient Optimization, and Multithreading. *Journal of Computational Chemistry*. 31(2): 455–461. https://doi.org/10.1002/jcc.21334.
[37] Zheng, C., X. Wu, R. Zeng, L. Lin, L. Xu, E. Li, and G. Dong. 2021. Computational Prediction of Hot Spots and Binding Site of Inhibitor NSC23766 on Rac1 Binding with Tiam1. *Frontiers in Chemistry*. 8: 625437. https://doi.org/10.3389/fchem.2020.625437.
[38] Goldin, A., J. M. Venditti, J. S. Macdonald, F. M. Muggia, J. E. Henney, and V. T. DeVita. 1981. Current Results of the Screening Program at the Division of Cancer Treatment, National Cancer Institute. *European Journal of Cancer*. 17(2): 129–142. https://doi.org/10.1016/0014-2964(81)90184-6.
[39] Li, C., W. Jia, J. Yang, C. Cheng, and O. E. Olaleye. 2022. Multi-Compound and Drug-Combination Pharmacokinetic Research on Chinese Herbal Medicines. *Acta Pharmacologica Sinica*. 43(12): 3080–3095. https://doi.org/10.1038/s41401-022-00924-z.
[40] Bickerton, G. R., G. V. Paolini, J. Besnard, S. Muresan, and A. L. Hopkins. 2012. Quantifying the Chemical Beauty of Drugs. *Nature Chemistry*. 4(2): 90–98. https://doi.org/10.1038/nchem.1243.
[41] Benet, L. Z., C. M. Hosey, O. Ursu, and T. I. Oprea. 2016. BDDCS, the Rule of 5 and Drugability. *Advanced Drug Delivery Reviews*. 101: 89–98. https://doi.org/10.1016/j.addr.2016.05.007.
[42] Arnott, J. A., and S. L. Planey. 2012. The Influence of Lipophilicity in Drug Discovery and Design. *Expert Opinion on Drug Discovery*. 7(10): 863–875. https://doi.org/10.1517/17460441.2012.714363.
[43] Hussain, S. M., M. S. Hussain, A. A. L., and N. Arif. 2016. Characterization of Isolated Bioactive Phytoconstituents from *Flacourtia indica* as Potential Phytopharmaceuticals—An *in Silico* Perspective. *Journal of Pharmacognosy and Phytochemistry*. 5 (6): 323–331.
[44] Ramchandani, S., I. Naz, N. Dhudha, and M. Garg. 2020. An Overview of the Potential Anticancer Properties of Cardamonin. *Exploration of Targeted Anti-Tumor Therapy*. 1(6): 413–426. https://doi.org/10.37349/etat.2020.00026.
[45] Zhang, H., T. Zhang, K. M. Saravanan, L. Liao, H. Wu, H. Zhang, H. Zhang, Y. Pan, X. Wu, and Y. Wei. 2022. DeepBindBC: A Practical Deep Learning Method for Identifying Native-Like Protein–Ligand Complexes in Virtual Screening. *Methods*. 205: 247–262. https://doi.org/10.1016/j.ymeth.2022.04.011.
[46] Joyner, P. M., D. P. Tran, M. A. Zenaidee, and J. A. Loo. 2022. Characterization of Protein–Ligand Binding Interactions of Enoyl-ACP Reductase (FabI) by Native MS Reveals Allosteric Effects of Coenzymes and the Inhibitor Triclosan. *Protein Science*. 31(3): 568–579. https://doi.org/10.1002/pro.4233.
[47] Ma, N., E. Xu, Q. Luo, and G. Song. 2023. Rac1: A Regulator of Cell Migration and a Potential Target for Cancer Therapy. *Molecules*. 28(7): 2976. https://doi.org/10.3390/molecules28072976.
[48] Zhou, X., J. Qian, L. Hua, Q. Shi, Z. Liu, Y. Xu, B. Sang, J. Mo, and R. Yu. 2013. Geranylgeranyltransferase I Promotes Human Glioma Cell Growth through Rac1 Membrane Association and Activation. *Journal of Molecular Neuroscience*. 49(1): 130–139. https://doi.org/10.1007/s12031-012-9910-7.
[49] Zhu, L., Y. Sun, Q. Wu, C. Zhang, and J. Ling. 2020. "CAPN6 Regulates Uterine Leiomyoma Cell Proliferation and Apoptosis through the Rac1-Dependent Signaling Pathway." *Annals of Clinical and Laboratory Science* 50 (1): 24–30.
[50] Bid, H. K., R. D. Roberts, P. K. Manchanda, and P. J. Houghton. 2013. RAC1: An Emerging Therapeutic Option for Targeting Cancer Angiogenesis and Metastasis. *Molecular Cancer Therapeutics*. 12(10): 1925–1934. https://doi.org/10.1158/1535-7163.MCT-13-0164.